Temporal Correlations for a Non-Stationary Vehicle-to-Vehicle Channel Model Allowing Velocity Variations

Qiuming Zhu, *Member, IEEE*, Weidong Li, Cheng-Xiang Wang, *Fellow, IEEE*, Dazhuan Xu, Ji Bian, Xiaomin Chen, and Weizhi Zhong

***Abstract*— By taking into account moving scatterers and velocity variations of terminals, a non-stationary vehicle-to-vehicle (V2V) channel model under non-line-of-sight (NLoS) scenarios is proposed. Under 2D non-isotropic scattering scenarios, the closed-form expression of the time-variant temporal correlation function (TCF) for the proposed model is derived and analyzed. The derived expression is a general solution and includes most of the existing results as special cases, i.e., stationary scenarios, constant velocities of terminals, or fixed scatterers. In addition, the derived TCF has a good agreement with the simulated and measured results.**

***Index Terms*— Vehicle-to-vehicle (V2V) channels, non-stationary channels, non-isotropic scattering scenarios, temporal correlation function (TCF), velocity variations.**

I. Introduction

VEHICLE-TO-VEHICLE (V2V) communication systems can effectively reduce the number of deaths, injuries, and material loss by building up communication links between vehicles, pedestrians, and road infrastructures. However, the increasing density of vehicles and movements of scatterers decrease the efficiency of V2V communication systems. For the development of future V2V communication systems and fifth generation (5G) communication systems [1], [2], a thorough understanding of propagation characteristics for underlying V2V channels is indispensable. Meanwhile, the mobilities of both terminals and scatterers result in channel characteristics varying rapidly [3], which are different from those of traditional fixed-to-mobile (F2M) channels [4], [5]. Measurement campaigns have also proved that the wide-sense stationary (WSS) assumption in stationary V2V channel models [6], [7] is only valid within a short distance, e.g., 4.5 m for line-of-sight (LoS) scenarios and 2.7 m for non-line-of-sight (NLoS) scenarios [5]. The non-stationary aspects should be taken into account in the future V2V channel modeling.

Several non-stationary V2V channel models can be found in [1], [2], [8]–[12]. However, the models in [8]–[10] assumed that both the mobile transmitter (MT) and mobile receiver (MR) moved with a fixed speed and direction. Under realistic V2V scenarios, vehicles may experience acceleration/deceleration due to different conditions. The authors in [11] and [12] took velocity variations into account, but they did not consider the movements of scatterers. However, the mobility of scatterers, i.e., other vehicles and pedestrians, increases the complexity of V2V communication systems and reduces the system performance due to the increased temporal correlation, which refers to the dependence of channel impulse response in the time domain [3], [10]. Thus, the exploitation of temporal correlations is vital to designing, optimizing and evaluating the V2V communication systems. It is worth mentioning that a closed-form expression of temporal correlation function (TCF) is vital to observe intuitively how movements of terminals and scatterers can affect the temporal correlations and get an explicit expression of system performance. However, the TCFs of aforementioned models were usually analyzed by simulations. This letter aims to fill these gaps. The major contributions and novelties are summarized as follows:

1) Based on Taylor series expansion, a closed-form expression of time-variant Doppler frequency under 2D V2V NLoS scattering scenarios is developed. Combing with the twin-cluster approach [14], [15], a general model for non-stationary V2V channels with moving scatterers and velocity variations of terminals is proposed. The new model can also be applied to fixed-to-fixed (F2F) and F2M channels by adjusting velocity parameters.

2) Under 2D non-isotropic von Mises (VM) scattering scenarios, a closed-form expression of TCF for the proposed model is derived. The derived result is an explicit function of time-variant velocity parameters, i.e., the speed and direction of MT, MR, and scatterers.

Manuscript received March 31, 2019; accepted April 25, 2019. Date of publication May 15, 2019; date of current version July 10, 2019. This work is supported by the Fundamental Research Funds for the Central Universities (Grant No. 2242019R30001), the Taishan Scholar Program of Shandong Province, the EU H2020 RISE TESTBED project (Grant No. 734325), National Key Scientific Instrument and Equipment Development Project (Grant No. 2013YQ200607), NSF of China (Grant No. 61827801), and Open Foundation for Graduate Innovation of NUAA (Grant No. KFJJ 20180408). The associate editor coordinating the review of this letter and approving it for publication was T. Han. *(Corresponding author: Cheng-Xiang Wang.)*

Q. Zhu, W. Li, D. Xu, and X. Chen are with the Key Laboratory of Dynamic Cognitive System of Electromagnetic Spectrum Space, College of Electronic and Information Engineering, Nanjing University of Aeronautics and Astronautics, Nanjing 211106, China (e-mail: zhuqiuming@nuaa.edu.cn; liweidong@nuaa.edu.cn; xudazhuan@nuaa.edu.cn; chenxm402@nuaa.edu.cn).

C.-X. Wang is with the National Mobile Communications Research Laboratory, School of Information Science and Engineering, Southeast University, Nanjing 211189, China, and also with Purple Mountain Laboratories, Nanjing 211111, China (e-mail: chxwang@seu.edu.cn).

J. Bian is with the Shandong Provincial Key Laboratory of Wireless Communication Technologies, School of Information Science and Engineering, Shandong University at Qingdao, Qingdao 266237, China (e-mail: bianjimail@163.com).

W. Zhong is with the Key Laboratory of Dynamic Cognitive System of Electromagnetic Spectrum Space, College of Astronautics, Nanjing University of Aeronautics and Astronautics, Nanjing 211106, China (e-mail: zhongwz@nuaa.edu.cn).

Digital Object Identifier 10.1109/LCOMM.2019.2916251

The remainder of this letter is organized as follows. Section II proposes a non-stationary V2V channel model. In Section III, the theoretical TCF of the proposed model under VM scattering scenarios is derived. The simulation results are performed and compared with the theoretical and measured ones in Section V. Finally, some conclusions are given in Section VI.

II. A Non-Stationary V2V Channel Model

Considering a typical V2V communication scenario, the MT and MR have time-variant velocities denoted as $\mathbf{v}^{\mathrm{MT}}(t)$ and $\mathbf{v}^{\mathrm{MR}}(t)$, respectively. The V2V channel includes several propagation paths and each path may contain several clusters. Note that the single-bounce and double-bounce cases can be viewed as two special cases of NLoS scenarios, i.e., one or two clusters existing along the certain path. Under NLoS scenarios, the first and last clusters are denoted by $\mathbf{S}_n^{\mathrm{MT}}$ and $\mathbf{S}_n^{\mathrm{MR}}$, respectively. $\mathbf{v}^{\mathrm{S}_n^i}(t)$, $i \in \{\mathrm{MT}, \mathrm{MR}\}$ is the time-variant velocity of MT and MR, $\mathbf{v}^{i,\mathrm{S}_n^i}(t) = \mathbf{v}^i(t) - \mathbf{v}^{\mathrm{S}_n^i}(t) = v^i(t)\mathrm{e}^{\mathrm{j}\alpha_v^i(t)}$ is the relative velocity between the MT and $\mathrm{S}_n^{\mathrm{MT}}$ or between the MR and $\mathrm{S}_n^{\mathrm{MR}}$, d_n^i is the initial distance between the MT and $\mathrm{S}_n^{\mathrm{MT}}$ or between the MR and $\mathrm{S}_n^{\mathrm{MR}}$, $\bar{\alpha}_n^i$ is the mean value of angle of arrival (AoD) or angle of departure (AoA). Note that all angle parameters are time-variant and related with the movements of terminals and scatterers [16].

Under non-stationary scattering environments, the time-variant channel impulse response (CIR) between the MT and MR can be expressed as [14]

$$h(t,\tau) = \sum_{n=1}^{N(t)} c_n(t) h_n(t) \delta(\tau - \tau_n(t)) \tag{1}$$

where $N(t)$ denotes the number of propagation paths, which are characterized by path delay $\tau_n(t)$, path gain $c_n(t)$, and normalized channel gain $h_n(t)$. In (1), $\tau_n(t)$ can be defined as $\tau_n^{\mathrm{MT}}(t) + \tau_n^{\mathrm{MR}}(t) + \tilde{\tau}_n(t)$, where $\tau_n^i(t)$ denotes the delays of first and last bounces, respectively, and $\tilde{\tau}_n(t)$ denotes the equivalent delay of virtual link. In addition, $h_n(t)$ can be further modeled by the summation of infinite sub-paths [14], [17], i.e.,

$$h_n(t) = \lim_{M\to\infty} \frac{1}{\sqrt{M}} \sum_{m=1}^{M} \mathrm{e}^{\mathrm{j}(2\pi \int_0^t f_{n,m}(t')\mathrm{d}t' + \theta_{n,m})} \tag{2}$$

where M denotes the number of sub-paths, $f_{n,m}(t)$ is the time-variant Doppler frequency, and the phase $\theta_{n,m} = \theta''_{n,m} + \theta'_{n,m}$ including the initial phase $\theta''_{n,m}$ and the accumulated phase $\theta'_{n,m} = \int_{-\infty}^{0} f_{n,m}(t')\mathrm{d}t'$. Since $\theta''_{n,m}$ is random and usually uniformly distributed over $[-\pi, \pi)$ and $\theta'_{n,m}$ is periodical over $[-\pi, \pi)$, $\theta_{n,m}$ can be expressed by an independent uniformly distributed random variable over $[-\pi, \pi)$.

Under NLoS scenarios, the rest of clusters between the first and last clusters can be abstracted by a virtual link [14]. Thus, the total Doppler frequency can be calculated by [4], [10]

$$\begin{aligned} f_{n,m}(t) = {} & \frac{\mathbf{v}^{\mathrm{MT}}(t)\tilde{\mathbf{r}}_{\mathrm{S}_{n,m}^{\mathrm{MT}},\mathrm{MT}}(t)}{\lambda} + \frac{\mathbf{v}^{\mathrm{S}_n^{\mathrm{MT}}}(t)\tilde{\mathbf{r}}_{\mathrm{MT},\mathrm{S}_{n,m}^{\mathrm{MT}}}(t)}{\lambda} \\ & + \frac{\mathbf{v}^{\mathrm{MR}}(t)\tilde{\mathbf{r}}_{\mathrm{S}_{n,m}^{\mathrm{MR}},\mathrm{MR}}(t)}{\lambda} + \frac{\mathbf{v}^{\mathrm{S}_n^{\mathrm{MR}}}(t)\tilde{\mathbf{r}}_{\mathrm{MR},\mathrm{S}_{n,m}^{\mathrm{MR}}}(t)}{\lambda} \end{aligned} \tag{3}$$

where $\tilde{\mathbf{r}}_{\mathrm{S}_{n,m}^i,i}$ and $\tilde{\mathbf{r}}_{i,\mathrm{S}_{n,m}^i}$ denote the unit direction vectors from $\mathrm{S}_{n,m}^i$ to i and from i to $\mathrm{S}_{n,m}^i$, respectively, and λ means the wavelength. Let us consider the relative velocity and rewrite (3) as

$$\begin{aligned} f_{n,m}(t) &= \frac{\mathbf{v}^{\mathrm{MT},\mathrm{S}_n^{\mathrm{MT}}}(t)\tilde{\mathbf{r}}_{\mathrm{S}_{n,m}^{\mathrm{MT}},\mathrm{MT}}(t)}{\lambda} + \frac{\mathbf{v}^{\mathrm{MR},\mathrm{S}_n^{\mathrm{MR}}}(t)\tilde{\mathbf{r}}_{\mathrm{S}_{n,m}^{\mathrm{MR}},\mathrm{MR}}(t)}{\lambda} \\ &= \frac{v^{\mathrm{MT},\mathrm{S}_n^{\mathrm{MT}}}(t)}{\lambda}\cos(\alpha_{n,m}^{\mathrm{MT}}(t) - \alpha_v^{\mathrm{MT},\mathrm{S}_n^{\mathrm{MT}}}(t)) \\ &\quad + \frac{v^{\mathrm{MR},\mathrm{S}_n^{\mathrm{MR}}}(t)}{\lambda}\cos(\alpha_{n,m}^{\mathrm{MR}}(t) - \alpha_v^{\mathrm{MR},\mathrm{S}_n^{\mathrm{MR}}}(t)) \\ &= f_{n,m}^{\mathrm{MT},\mathrm{S}_n^{\mathrm{MT}}}(t) + f_{n,m}^{\mathrm{MR},\mathrm{S}_n^{\mathrm{MR}}}(t) \end{aligned} \tag{4}$$

where $f_{n,m}^{i,\mathrm{S}_n^i}(t)$, $i \in \{\mathrm{MT}, \mathrm{MR}\}$ represents the Doppler frequency occurs at the MT or MR, and $\alpha_{n,m}^i(t)$ denotes the AoA or AoD of the mth sub-path within the nth path.

In order to make the model of Doppler frequency more tractable, the speed and movement direction can be approximated by two linear functions over the short analytical time interval, i.e., $v^i(t) = v_0^i + a_0^i t$ and $\alpha_v^i(t) = \alpha_v^i + b_0^i t$ [11], where a_0^i and b_0^i represent the corresponding accelerations, respectively. Then, we expand $\cos(\alpha_{n,m}^i(t) - \alpha_v^i(t))$ by Taylor series expansion as

$$\cos(\alpha_{n,m}^i(t) - \alpha_v^i(t)) = \cos(\alpha_{n,m}^i - \alpha_v^i) + c_0^i \cdot t + \frac{c_1^i}{2} \cdot t^2 + \cdots. \tag{5}$$

It can be proved that the first two terms can approximate the whole one quite well and c_0^i can be expressed as

$$c_0^i = -\frac{v_0^i \sin^2(\alpha_{n,m}^i - \alpha_v^i)}{d_n^i} + b_0^i \cdot \sin(\alpha_{n,m}^i - \alpha_v^i) \tag{6}$$

where d_n^i, $i \in \{\mathrm{MT}, \mathrm{MR}\}$ denotes the initial distance between the MT and $\mathrm{S}_n^{\mathrm{MT}}$ or between the MR and $\mathrm{S}_n^{\mathrm{MR}}$, $\alpha_{n,m}^i$ is the initial value of AoD or AoA, and α_v^i means the initial speed of the MT or MR. Finally, the Doppler frequency can be modeled by

$$\begin{aligned} f_{n,m}^{i,\mathrm{S}_n^i}(t) \approx {} & \frac{a_0^i c_0^i t^2}{\lambda} + \frac{a_0^i \cdot \cos(\alpha_{n,m}^i - \alpha_v^i) + v_0^i c_0^i}{\lambda} t \\ & + \frac{v_0^i \cos(\alpha_{n,m}^i - \alpha_v^i)}{\lambda} \end{aligned} \tag{7}$$

which explicitly reveals the impact of time-variant movement parameters of terminals and clusters. It's worth mentioning that the authors in [17] assumed the Doppler frequency changing linearly and derived $f_{n,m}^{i,\mathrm{S}_n^i}(t)$ by using its first-order Taylor expansion. Under this assumption, the channel gain $h_n(t)$ can be modeled by the sum of linear frequency modulated signals (SoLFM) [13] or sum of chirp signals (SoC_h) [17]. In contrast, by substituting (7) and (4) into (2), $h_n(t)$ in this letter can be expressed as

$$h_n(t) = \lim_{M\to\infty} \frac{1}{\sqrt{M}} \sum_{m=1}^{M} e^{\mathrm{j}(2\pi(A\cdot t^3 + B\cdot t^2 + C\cdot t) + \theta_{n,m})} \tag{8}$$

$$\rho_n(t,\Delta t)=\int_{-\pi}^{\pi}\int_{-\pi}^{\pi} \mathrm{e}^{-\mathrm{j}2\pi\int_t^{t+\Delta t} f_{n,m}(t')\mathrm{d}t'}\cdot\sqrt{p_{\alpha_{n,m}^{\mathrm{MT}},\alpha_{n,m}^{\mathrm{MR}}}(\alpha_n^{\mathrm{MT}}(t),\alpha_n^{\mathrm{MR}}(t))}\cdot\sqrt{p_{\alpha_{n,m}^{\mathrm{MT}},\alpha_{n,m}^{\mathrm{MR}}}(\alpha_n^{\mathrm{MT}}(t+\Delta t),\alpha_n^{\mathrm{MR}}(t+\Delta t))}\mathrm{d}\alpha_n^{\mathrm{MT}}\mathrm{d}\alpha_n^{\mathrm{MR}} \tag{11}$$

$$\rho_n^i(t,\Delta t) = \frac{\mathrm{I}_0\left(\sqrt{{\kappa^i}^2-{D_n^i}^2-{E_n^i}^2+2\mathrm{j}\cdot\kappa^i\cdot\left(D_n^i\cdot\cos\left(\left(\frac{v_0^i\cdot\sin(\bar{\alpha}_n^i-\alpha_v^i)}{d_n^i}-b_0^i\right)\cdot t+\bar{\alpha}_n^i-\alpha_v^i\right)+E_n^i\cdot\sin\left(\left(\frac{v_0^i\cdot\sin(\bar{\alpha}_n^i-\alpha_v^i)}{d_n^i}-b_0^i\right)\cdot t+\bar{\alpha}_n^i-\alpha_v^i\right)\right)}\right)}{\mathrm{I}_0(\kappa^i)} \tag{16}$$

where

$$A = -\frac{a_0^{\mathrm{MT}}v_0^{\mathrm{MT}}\sin^2(\alpha_{n,m}^{\mathrm{MT}}-\alpha_v^{\mathrm{MT}})}{3\lambda d_n^{\mathrm{MT}}} \frac{-a_0^{\mathrm{MR}}v_0^{\mathrm{MR}}\sin^2(\alpha_{n,m}^{\mathrm{MR}}-\alpha_v^{\mathrm{MR}})}{3\lambda d_n^{\mathrm{MR}}} \tag{9a}$$

$$B = \frac{a_0^{\mathrm{MT}}\cdot\cos(\alpha_{n,m}^{\mathrm{MT}}-\alpha_v^{\mathrm{MT}})+v_0^{\mathrm{MT}}b_0^{\mathrm{MT}}}{2\lambda} + \frac{a_0^{\mathrm{MR}}\cdot\cos(\alpha_{n,m}^{\mathrm{MR}}-\alpha_v^{\mathrm{MR}})+v_0^{\mathrm{MR}}b_0^{\mathrm{MR}}}{2\lambda} \tag{9b}$$

$$C = \frac{v_0^{\mathrm{MT}}\cos(\alpha_{n,m}^{\mathrm{MT}}-\alpha_v^{\mathrm{MT}})}{\lambda}+\frac{v_0^{\mathrm{MR}}\cos(\alpha_{n,m}^{\mathrm{MR}}-\alpha_v^{\mathrm{MR}})}{\lambda}. \tag{9c}$$

Finally, our proposed V2V channel model can be obtained by substituting the new Doppler frequency model of (8) and (9) into (1). Note that our model can be easily extended to multiple-input multiple-output (MIMO) channels, while this letter only focuses on single-input single-output (SISO) channels and their temporal correlation properties.

III. TCF of Proposed Model Under Non-Isotropic Scenarios

The normalized TCF of the nth path for non-stationary V2V channels should be time-variant and can be defined as

$$\rho_n(t,\Delta t)=\mathrm{E}[h_n(t)h_n^*(t+\Delta t)]_{\{\alpha_{n,m}^{\mathrm{MT}}(t),\alpha_{n,m}^{\mathrm{MR}}(t),\theta_{n,m}\}} \tag{10}$$

where the expectation function $\mathrm{E}[\cdot]$ applies to the random variables such as $\alpha_n^{\mathrm{MT}}(t)$, $\alpha_n^{\mathrm{MR}}(t)$ and $\theta_{n,m}$. By substituting (2) into (10) and averaging over $\theta_{n,m}$, it yields (11), as shown at the top of this page, and $p_{\alpha_{n,m}^{\mathrm{MT}},\alpha_{n,m}^{\mathrm{MR}}}(\alpha_n^{\mathrm{MT}}(t),\alpha_n^{\mathrm{MR}}(t))$ denotes the time-variant joint distribution of random angles. Note that (11) is suitable for both LoS and NLoS scenarios. For example, it reduces to the LoS condition by setting $\alpha_n^{\mathrm{MT}}(t)=\pi-\alpha_n^{\mathrm{MR}}(t)$ as well as the single-bounce condition by using geometrical relationships between the AoD and AoA. For general multi-bounce NLoS scenarios, the AoA and AoD are usually assumed independent and their distributions could be obtained by measurement campaigns separately. Under this condition, it follows from (11) that the TCF can be expressed as

$$\rho_n(t,\Delta t)=\rho_n^{\mathrm{MT}}(t,\Delta t)\rho_n^{\mathrm{MR}}(t,\Delta t) \tag{12}$$

where $\rho_n^i(t,\Delta t), i\in\{\mathrm{MT},\mathrm{MR}\}$ represents the TCF at the MT or MR and can be further calculated by

$$\rho_n^i(t,\Delta t) = \int_{-\pi}^{\pi}\mathrm{e}^{-\mathrm{j}2\pi\int_t^{t+\Delta t}f_{n,m}^i(t')\mathrm{d}t'} \cdot\sqrt{p_{\alpha_{n,m}^i}(\alpha_n^i(t))}\cdot\sqrt{p_{\alpha_{n,m}^i}(\alpha_n^i(t+\Delta t))}\mathrm{d}\alpha_n^i. \tag{13}$$

In order to quantificationally investigate temporal correlations of our proposed model, we assume the AoA and AoD follow the VM distribution. This distribution is flexible and can be used to approximate many distributions, e.g., uniform and Gaussian. Based on the measured data, the authors in [3] and [11] employed it to describe the signal angles under non-isotropic scattering conditions. The VM probability distribution function (PDF) is given by

$$P_{\alpha_{n,m}^i}(\alpha_n^i)=\frac{\exp\left(\kappa^i\cos(\alpha_n^i-\bar{\alpha}_n^i)\right)}{2\pi\mathrm{I}_0(\kappa^i)} \tag{14}$$

where $\mathrm{I}_0(\cdot)$ is the zeroth-order modified Bessel function of the first kind, $\kappa^i>0$ and $\bar{\alpha}_n^i$ denote the distribution factor and the mean value of angles, respectively. Since κ^i is almost constant during short analytical time intervals (several tens of milliseconds), angle offsets can be approximately time-invariant, i.e., $\alpha_n^i(t+\Delta t)-\bar{\alpha}_n^i(t+\Delta t)\approx\alpha_n^i(t)-\bar{\alpha}_n^i(t)$. Holding this condition and substituting (8) and (14) into (13), it yields

$$\rho_n^i(t,\Delta t) = \frac{1}{2\pi\mathrm{I}_0(\kappa^i)}\int_{-\pi}^{\pi}\mathrm{e}^{\kappa^i\cos(\alpha_n^i(t)-\bar{\alpha}_n^i(t))} \cdot\mathrm{e}^{-\mathrm{j}\frac{2\pi}{\lambda}\int_t^{t+\Delta t}(\frac{a_0^ib_0^i}{3}\cdot t'^2+\frac{a_0^i\cdot\cos(\alpha_n^i-\alpha_v^i)+v_0^ib_0^i}{2}\cdot t')\mathrm{d}t'} \cdot\mathrm{e}^{-\frac{\mathrm{j}\cdot2\pi v_0^i\cos(\alpha_n^i-\alpha_v^i)\cdot\Delta t}{\lambda}}\mathrm{d}\alpha_n^i. \tag{15}$$

By using [18. eq. (3.338-4)], we can obtain the closed-form expression of TCF as (16), shown at the top of this page, where

$$D_n^i = \frac{2\pi}{\lambda}\cdot\left(\frac{v^i(t)\Delta t}{2}+\frac{a_0^i\Delta t^2}{6}\right)+\frac{2\pi}{\lambda}\cdot\left(\frac{v^i(t)\Delta t}{2}+\frac{a_0^i\Delta t^2}{3}\right) \cdot\cos\left(\left(\frac{v_0^i\cdot\sin(\bar{\alpha}_n^i-\alpha_v^i)}{d_n^i}-b_0^i\right)\cdot\Delta t\right) \tag{17a}$$

$$E_n^i = \frac{2\pi}{\lambda}\cdot\left(\frac{v^i(t)\Delta t}{2}+\frac{a_0^i\Delta t^2}{3}\right) \cdot\sin\left(\left(\frac{v_0^i\cdot\sin(\bar{\alpha}_n^i-\alpha_v^i)}{d_n^i}-b_0^i\right)\cdot\Delta t\right). \tag{17b}$$

TABLE I
DETAILED VELOCITY PARAMETERS

scenario	v_0^i (m/s)	a_0^i (m/s^2)	b_0^i (s^{-1})	α_v^i
outdoor	$v_0^{\mathrm{MT}}=1.5$	$a_0^{\mathrm{MT}}=1$	$b_0^{\mathrm{MT}}=0$	$\alpha_v^{\mathrm{MT}}=\frac{\pi}{3}$
	$v_0^{\mathrm{MR}}=1.5$	$a_0^{\mathrm{MR}}=1.5$	$b_0^{\mathrm{MR}}=\frac{\pi}{12}$	$\alpha_v^{\mathrm{MR}}=\frac{\pi}{6}$
indoor	$v_0^{\mathrm{MT}}=0.6$	$a_0^{\mathrm{MT}}=0$	$b_0^{\mathrm{MT}}=0$	$\alpha_v^{\mathrm{MT}}=\frac{\pi}{2}$
	$v_0^{\mathrm{MR}}=0.6$	$a_0^{\mathrm{MR}}=0$	$b_0^{\mathrm{MR}}=0$	$\alpha_v^{\mathrm{MR}}=\frac{\pi}{2}$

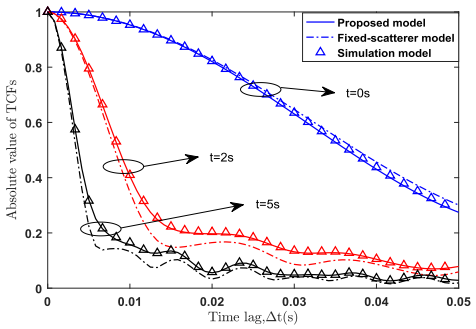

Fig. 1. Absolute values of the TCFs of different models at different time instants (outdoor NLoS scenario, $d_n^i \sim \mathrm{U}(5,30)$ m, $\left\|\mathbf{v}^{\mathrm{S}_n^i}(t)\right\| \sim \mathrm{U}(0,1)$ m/s, and $\alpha_v^{\mathbf{S}_n^i}(t) \sim \mathrm{U}(-\pi,\pi)$).

Finally, by substituting (16) into (12), the closed-form TCF for the proposed V2V channel model can be obtained.

It should be mentioned that the derived TCF can clearly reveal the influence of the movements of terminals and scatterers via v_0^i, α_v^i, a_0^i and b_0^i. Moreover, this expression is a general solution and includes many existing results for stationary and non-stationary channels. For example, by setting $\kappa^i = 0$, $a_0^i = 0$, $b_0^i = 0$ and $\bar{\alpha}_n^i = \alpha_v^i$, the derived TCF reduces to the classic result under isotropic scattering conditions as [20. eq. (35)]. For non-isotropic scattering scenarios, by setting $a_0^i = 0$, $b_0^i = 0$, $\alpha_v^i = 0$ and $\bar{\alpha}_n^i(t) = \bar{\alpha}_n^i(t+\Delta t)$, it has the same form with [19. eq. (20)]. Moreover, it's also equivalent to the result of [11. eq. (42)] as long as all scatterers are fixed and the time-variant angles $\alpha_n^i(t)$ are time independent.

IV. RESULTS AND ANALYSIS

In this section, the impacts of velocity variations and moving scatterers on the TCF are investigated and validated. Firstly, we consider an outdoor NLoS scenario with the AoA and AoD following the VM distribution ($\kappa = 1$). The carrier frequency is 2.48 GHz. The scatterers with random velocities are assumed to distribute uniformly around the MT and MR. The terminals have different initial velocities and accelerations as shown in Table I. The absolute values of TCFs at three time instants, i.e., t = 0 s, 2 s, and 5 s are compared in Fig. 1. Here, the theoretical TCFs of our model are obtained by (16) and (12), while the ones of the model with fixed scatterers can be calculated by [11. eq. (42)]. In order to verify

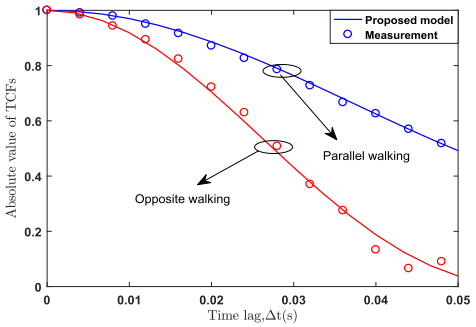

Fig. 2. Absolute values of derived and measured TCFs at different time instants (indoor NLoS scenario, $d_n^i \sim \mathrm{U}(5,10)$ m, $\left\|\mathbf{v}^{\mathrm{S}_n^i}(t)\right\| \sim \mathrm{U}(0,1)$ m/s, and $\alpha_v^{\mathbf{S}_n^i}(t) \sim \mathrm{U}(-\pi,\pi)$).

the correctness of derivations, we also simulate 10^7 channel fading samples by (8) and demonstrate the simulated TCFs in Fig. 1. As we can see that the simulated TCFs match well with the theoretical ones of our model. However, the TCFs of the model excluding moving scatterers are quite different with ours, which means that the moving scatterers do have influence on TCFs especially when the time lag increases. Finally, it also shows in Fig. 1 velocity variations have a great impact on time correlations. In addition, when the computer is configured with i5-4210M CPU and 4 GB RAM, it takes 3.78 s to obtain the simulated TCFs in Fig. 1, while it takes only 0.99 s by using the derivations.

It is worth mentioning that our proposed model and the derived TCF can also be applied to the mobile-to-mobile (M2M) channel, e.g. the model in [4], where the receiver and transmitter are presented by two moving human. In [4], the authors performed channel measurement campaigns in a NLoS indoor office with moving scatterers. The TCFs for two straight linear trajectories, i.e., parallel and opposite walking, were measured at 2.48 GHz. These measurement results can be used to verify the effectiveness of our model and the derived TCF as well. By setting the same parameters and substituting $v_0^{\mathrm{MT}} = v_0^{\mathrm{MR}} = 0.6$ m/s, $\alpha_v^{\mathrm{MT}} = \alpha_v^{\mathrm{MR}} = \pi/2$, $a_0^{\mathrm{MT}} = a_0^{\mathrm{MR}} = 0$ m/s^2, $b_0^{\mathrm{MT}} = b_0^{\mathrm{MR}} = 0$ s^{-1} and $\kappa = 0$ into (15), the absolute values of theoretical and measured TCFs under these two measurement scenarios are compared in Fig. 2. The good agreement between measured and theoretical TCFs shows the usefulness of both the proposed model and theoretical derivations.

V. CONCLUSIONS

We have proposed a new non-stationary V2V channel model allowing for velocity variations of terminals as well as moving scatterers. Based on the proposed model, the closed-form expression of TCF under non-isotropic scattering environments has been derived and verified by simulations and measurements. The derived theoretical TCF includes many existing results as special cases. In addition, it clearly reveals the impact of velocities on TCFs, which is helpful for the performance evaluation and optimization of V2V communication systems under realistic conditions.

REFERENCES

[1] C.-X. Wang, J. Bian, J. Sun, W. Zhang, and M. Zhang, "A survey of 5G channel measurements and models," *IEEE Commun. Surveys Tuts.*, vol. 20, no. 4, pp. 3142–3168, 4th Quart., 2018.

[2] S. Wu, C.-X. Wang, E.-H. M. Aggoune, M. M. Alwakeel, and X. You, "A general 3-D non-stationary 5G wireless channel model," *IEEE Trans. Commun.*, vol. 66, no. 7, pp. 3065–3078, Jul. 2018.

[3] A. G. Zajić, "Impact of moving scatterers on vehicle-to-vehicle narrow-band channel characteristics," *IEEE Trans. Veh. Technol.*, vol. 63, no. 7, pp. 3094–3106, Sep. 2014.

[4] G. Makhoul, F. Mani, R. D'Errico, and C. Oestges, "On the modeling of time correlation functions for mobile-to-mobile fading channels in indoor environments," *IEEE Antennas Wireless Propag. Lett.*, vol. 16, pp. 549–552, Mar. 2017.

[5] R. He *et al.*, "Vehicle-to-vehicle radio channel characterization in crossroad scenarios," *IEEE Trans. Veh. Technol.*, vol. 65, no. 8, pp. 5850–5861, Aug. 2016.

[6] M. Patzold, B. O. Hogstad, and N. Youssef, "Modeling, analysis, and simulation of MIMO mobile-to-mobile fading channels," *IEEE Trans. Wireless Commun.*, vol. 7, no. 2, pp. 510–520, Feb. 2008.

[7] Y. Yuan, C.-X. Wang, X. Cheng, B. Ai, and D. I. Laurenson, "Novel 3D geometry-based stochastic models for non-isotropic MIMO vehicle-to-vehicle channels," *IEEE Trans. Wireless Commun.*, vol. 13, no. 1, pp. 298–309, Jan. 2014.

[8] Y. Yuan, C.-X. Wang, Y. He, M. M. Alwakeel, and E. M. Aggoune, "3D wideband non-stationary geometry-based stochastic models for non-isotropic MIMO vehicle-to-vehicle channels," *IEEE Trans. Wireless Commun.*, vol. 14, no. 12, pp. 6883–6895, Dec. 2015.

[9] C. A. Gutiérrez, J. T. Gutiérrez-Mena, J. M. Luna-Rivera, D. U. Campos-Delgado, R. Velázquez, and M. Pätzold, "Geometry-based statistical modeling of non-WSSUS mobile-to-mobile Rayleigh fading channels," *IEEE Trans. Veh. Technol.*, vol. 67, no. 1, pp. 362–377, Jan. 2018.

[10] A. Borhani and M. Pätzold, "Correlation and spectral properties of vehicle-to-vehicle channels in the presence of moving scatterers," *IEEE Trans. Veh. Technol.*, vol. 62, no. 9, pp. 4228–4239, Nov. 2013.

[11] W. Dahech, M. Pätzold, C. A. Gutiérrez, and N. Youssef, "A non-stationary mobile-to-mobile channel model allowing for velocity and trajectory variations of the mobile stations," *IEEE Trans. Wireless Commun.*, vol. 16, no. 3, pp. 1987–2000, Mar. 2017.

[12] R. He, B. Ai, G. L. Stüber, and Z. Zhong, "Mobility model-based non-stationary mobile-to-mobile channel modeling," *IEEE Trans. Wireless Commun.*, vol. 17, no. 7, pp. 4388–4400, Jul. 2018.

[13] X. Liu, Q. Zhu, X. Chen, and K. Jiang, "A new simulation model for non-stationary fading channel," in *Proc. 3rd ICED*, Phuket, Thailand, Aug. 2016, pp. 66–69.

[14] Q. Zhu *et al.*, "A novel 3D non-stationary wireless MIMO channel simulator and hardware emulator," *IEEE Trans. Commun.*, vol. 66, no. 9, pp. 3865–3878, Sep. 2018.

[15] H. Hofstetter, A. F. Molisch, and N. Czink, "A twin-cluster MIMO channel model," in *Proc. Antennas Propag. (EuCAP)*, Nice, France, Nov. 2006, pp. 1–8.

[16] J. Li, D. Jiang, and X. Zhang, "DOA estimation based on combined unitary ESPRIT for coprime MIMO radar," *IEEE Commun. Lett.*, vol. 21, no. 1, pp. 96–99, Jan. 2017.

[17] M. Paetzold and C. A. Gutierrez, "Definition and analysis of quasi-stationary intervals of mobile radio channels—Invited paper," in *Proc. IEEE VTC Spring*, Porto, Portugal, Jun. 2018, pp. 1–6.

[18] I. S. Gradshteĭn and I. M. Ryžhik, *Table of Integrals, Series, and Products*. New York, NY, USA: Academic, 2014.

[19] R. Parra-Michel, J. V. Castillo, L. R. Vela-Garcia, V. Kontorovich, and F. Peña-Campos, "A channel model and simulation technique for reproducing channel realizations with predefined stationary or non-stationary PSD," *IEEE Trans. Wireless Commun.*, vol. 17, no. 8, pp. 5409–5424, Aug. 2018.

[20] A. S. Akki and F. Haber, "A statistical model of mobile-to-mobile land communication channel," *IEEE Trans. Veh. Technol.*, vol. VT-35, no. 1, pp. 2–7, Feb. 1986.